Available online at www.sciencedirect.com
ScienceDirect
Energy Reports 9 (2023) 314–323
www.elsevier.com/locate/egyr

2022 The 3rd International Conference on Power and Electrical Engineering (ICPEE 2022)
29–31 December, Singapore

State and fault estimation scheme based on sliding mode observer for a Lithium-ion battery

Mokhtar Mohamed[a,*], Iestyn Pierce[a], Truong Quang Dinh[b]

[a] School of Computer Science and Electronic Engineering, Bangor University, Bangor, LL57 1UT, UK
[b] Warwick Manufacturing Group, University of Warwick, Coventry, CV4 7AL, UK

Received 24 April 2023; accepted 19 May 2023
Available online xxxx

Abstract

In electric vehicles, voltage and temperature sensors installed at the battery cell level or pack level are crucial for providing accurate information so the battery management system (BMS) can perform its functions properly. In this paper, a model-based sensor fault estimation scheme using a sliding mode technique has been proposed. Voltage and temperature models have been developed for a Lithium-ion battery cell. Then, a sliding mode observer has been proposed to estimate the systems' states as well as sensors fault signals independently and simultaneously. Nissan Leaf Gen4 2018 Lithium-ion cells have been selected to evaluate the performance of the proposed estimation scheme. Simulation results under different test scenarios have confirmed the feasibility and effectiveness of the developed method.

Peer-review under responsibility of the scientific committee of the 3rd International Conference on Power and Electrical Engineering, ICPEE, 2022.

Keywords: Lithium-ion batteries; State estimation; Fault estimation; Sliding mode observer

1. Introduction

Lithium-ion (Li-ion) batteries being promising solutions for energy storage applications such as electric vehicles (EVs) due to their high energy and power density, and long service [1–3]. However, recently many accidents associate with them raise a real concern about the safety and reliability [4,5]. A battery management system (BMS) plays a vital role in EVs for real-time monitoring of battery states to maintain the safe and effective operation of batteries. The key functions of the BMS are to periodically adjust the charge of individual cells to match the rest of the pack, states estimations (such as state of charge (SOC), state of health (SOH)), fault diagnosis and other advanced control features [6]. The poor performance of BMS due to misinformation provided by faulty sensors might lead to over-discharging & overcharging and estimation errors. All can result in thermal runaway events and then possible catastrophic consequences [7,8]. To ensure that BMS works efficiently and to avoid any serious

* Corresponding author.
E-mail addresses: m.mohamed@bangor.ac.uk, m_s_khalifa@yahoo.co.uk (M. Mohamed).

https://doi.org/10.1016/j.egyr.2023.05.086

Peer-review under responsibility of the scientific committee of the 3rd International Conference on Power and Electrical Engineering, ICPEE, 2022.

safety issues, fault diagnosis schemes are needed. Fault detection and isolation (FDI) could be one of techniques to increase safety and reliability in Li-ion batteries applications. The purpose of FDI is to detect any fault once occurs and determine the location of the fault. However, for a fault fault-tolerant control design, the information such as a magnitude is very useful. Hence a fault reconstruction and estimation (FRE) scheme is required to stabilises the closed-loop system and achieve the desired performance [9,10].

It is well known that sliding-mode control techniques exhibit high robustness and insensitivity to the so-called matched uncertainty [11]. Sliding mode observers (SMOs) based approaches have been widely used to develop FDI, particularly, FRE schemes [12,13]. Model-based fault diagnostic scheme that uses sliding mode observers designed based on the electrical and thermal dynamics of the battery is presented in [14] to develop sensors faults estimation schemes. The equivalent output errors are extracted on the sliding manifolds, then, residual signals are generated to detect, isolate, and estimate the sensor faults under the assumption that the faults and their time derivatives are bounded and finite. Moreover, it is assumed that no multiple faults can occur at the same time. Model-based sensor FDI scheme using an adaptive extended Kalman method to estimate the battery output voltage for a series battery pack is presented in [15]. The residual signals are generated by comparing between the estimated output voltage of the model with actual measurement values of the battery cell. However, this FDI mechanism is proposed based on the assumption that the most possibly being over-charged and over-discharged cells (two cells in a series battery pack) are vulnerable to sensor faults, and the rest of the cells and their sensors are working normally. Model-based sensor FDI scheme for a Li-ion cell is developed in [16] using a recursive least squares (RLS) method to estimate the equivalent circuit model (ECM) parameters in real time. Then, by applying a weighted moving average filter coupled with a cumulative sum control chart to detect any sensor faults. In [17], the SOC and capacity are estimated by the unscented Kalman filter (UKF). The residuals are compared with the constant threshold to identify faults of current or voltage sensors for the battery pack. The temperature sensor is assumed to be fault-free, which is used to distinguish the fault of a current or voltage sensor from the fault of a battery cell.

The aforementioned sensor fault diagnosis schemes and others that proposed for battery applications have one or more of the following issues. First, they aim to detect one fault at one time. Second, they ignored the temperature sensor fault. Third, only suitable for the battery pack. In this paper, a sensor fault scheme using a sliding mode observer is proposed for a battery system. The proposed technique is developed to estimate system states and sensor faults simultaneously, and it is applicable to be implemented for battery voltage model and battery thermal model independently. In this way, the detection of voltage sensor and temperature sensor faults can be achieved independently and simultaneously. The main contributions include:

- A generic estimation scheme directly applicable to estimate system states and sensor faults simultaneously.
- More than one fault can be estimated at one time.
- The proposed technique is applicable to be implemented for battery voltage model and battery thermal model independently for one battery as well as battery pack.

The main idea of this paper as explained in Fig. 1 is to apply the developed observer for both voltage and thermal models of the battery cell independently and simultaneously. The observer is developed to estimate thermal cell model states (i.e surface temperature and core temperature) [18], and to estimate voltage cell model states as explained in [19]. In addition, to estimate a sensor fault signal for both a surface temperature sensor and a terminal voltage sensor. The fault signal estimation is needed for designing a fault-tolerant control (FTC) which is out of the scope of this paper and considered as a future work.

2. System description and preliminaries

Consider a system described as follows

$$\dot{x} = \bar{A}x + \bar{B}u \tag{1}$$

$$y = \bar{C}x + \bar{D}f_s(t) \tag{2}$$

where $x \in R^n, u \in R^m$ and $y \in R^p$ with $m \leq p \leq n$ are the state variables, inputs and outputs of the system, respectively. The matrix triples $(\bar{A}, \bar{B}, \bar{C})$ are constant with appropriate dimensions, and $\bar{C}$ is of full rank. $\bar{D} \in R^{p\times q}(q \leq p)$ is a known sensor fault distribution matrix which has full column rank, and $f_s(t)$ is a sensor fault.

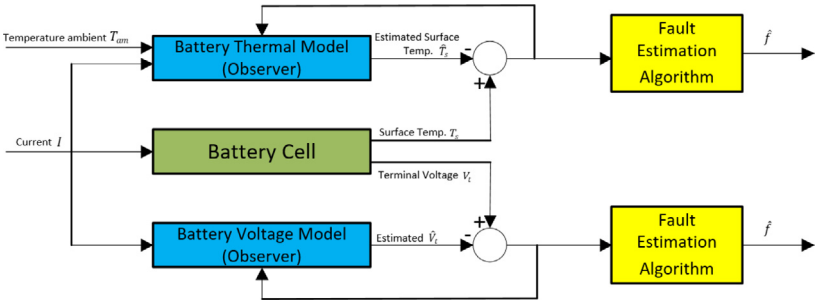

Fig. 1. System states estimation and fault diagnosis scheme.

For the simplicity, we assume that the matrix $\bar{D}$ has the following structure

$$\bar{D} = \begin{bmatrix} 0 \\ D_2 \end{bmatrix} \tag{3}$$

where $D_2 \in R^{q\times q}$. Moreover, since the matrix $\bar{C}$ is of full rank, there exists a non-singular matrix T_c such that

$$A = \begin{bmatrix} A_1 & A_2 \\ A_3 & A_4 \end{bmatrix} := T_c \bar{A} T_c^{-1} \tag{4}$$

$$B = \begin{bmatrix} B_1 \\ B_2 \end{bmatrix} := T_c \bar{B}, \text{ and } C = \begin{bmatrix} 0 & I_p \end{bmatrix} := \bar{C} T_c^{-1} \tag{5}$$

where $A_1 \in R^{(n-p)\times(n-p)}$, $B_1 \in R^{(n-p)\times m}$and $B_2 \in R^{p\times m}$. Thus in the new coordinates $(x_1 x_2)^T = T_c x$, the system can be written as

$$\dot{x}_1 = A_1 x_1 + A_2 x_2 + B_1 u \tag{6}$$

$$\dot{x}_2 = A_3 x_1 + A_4 x_2 + B_2 u \tag{7}$$

$$y = x_2 + D_2 f_s(t) \tag{8}$$

Assumption 1. It is assumed that f_s and $\dot{f}_s$ are both bounded, namely $\|f_s\| \le \beta_1$ and $\left\|\dot{f}_s\right\| \le \beta_2$ where β_1 and β_2 are known positive constants.

Assumption 2. The matrix pair (A, C) in (4)–(5) is observable.

From Assumption 2, there exist matrix L such that $A - LC$ is Hurwitz stable. This implies that, for any positive-definite matrix $Q \succ 0$, the Lyapunov equation

$$(A - LC)^T P + P(A - LC) = -Q \tag{9}$$

has unique positive-definite solution $P \succ 0$.

For further analysis, introduce partitions of P and Q which are conformable with the decomposition in (6)–(8) as follows

$$P = \begin{bmatrix} P_1 & P_2 \\ P_3 & P_4 \end{bmatrix}, Q = \begin{bmatrix} Q_1 & Q_2 \\ Q_3 & Q_4 \end{bmatrix} \tag{10}$$

where $P_1 \in R^{(n-p)\times(n-p)}$ and $Q_1 \in R^{(n-p)\times(n-p)}$. The following result is required for further analysis.

Lemma 1. *The matrix $A_1 + LA_3$ is Hurwitz stable, where $L = P_1^{-1} P_2$ and $L \in R^{(n-p)\times p}$, and P_1 & P_2 are defined in (10) and A_1 & A_2 are defined in (4), if the Lyapunov equation in (9) is satisfied.*

Proof. See Lemma 2.1 in [20].

3. Sliding mode observer design

In this section, a SMO is proposed to estimate system states and fault signals. Consider the system in (6)–(8) with no sensor fault. Introduce a linear coordinate transformation

$$z = \underbrace{\begin{bmatrix} I_{n-p} & L \\ 0 & I_p \end{bmatrix}}_{T} x \tag{11}$$

where L is defined in Lemma 1. In the new coordinate system z

$$\dot{z}_1 = (A_1 + LA_3)z_1 + (A_2 - A_1L) + L(A_4 - A_3L)z_2 + (B_1 + LB_2)u \tag{12}$$

$$\dot{z}_2 = A_3z_1 + (A_4 - A_3L)z_2 + B_2u \tag{13}$$

$$y = z_2 \tag{14}$$

For system (12)–(14), consider a dynamical system

$$\dot{\hat{z}}_1 = (A_1 + LA_3)\hat{z}_1 + (A_2 - A_1L) + L(A_4 - A_3L)y + (B_1 + LB_2)u + H(y - \hat{y}) + K_1v \tag{15}$$

$$\dot{\hat{z}}_2 = A_3\hat{z}_1 + (A_4 - A_3L)y + B_2u + K_2(y - \hat{y}) + K_3v \tag{16}$$

$$\hat{y} = \hat{z}_2 \tag{17}$$

where K_1, K_2 and K_3 will be defined later over the paper, and

$$v = sgn(y - \hat{y}) \tag{18}$$

If the state estimation errors are defined as $e_1 = z_1 - \hat{z}_1$, and $e_2 = z_2 - \hat{z}_2$. Then from (12)–(14) and (15)–(17), the error dynamics can be described by

$$\dot{e}_1 = (A_1 + LA_3)e_1 + He_2 - K_1v \tag{19}$$

$$\dot{e}_2 = A_3e_1 - K_2e_2 - K_3v \tag{20}$$

For convenience $\tilde{A}_1 = (A_1 + LA_3)$.

$$\dot{e}_1 = \tilde{A}_1e_1 + He_2 - K_1v \tag{21}$$

$$\dot{e}_2 = A_3e_1 - K_2e_2 - K_3v \tag{22}$$

Now consider the case after the occurrence of any sensor fault. From Eq. (8), and therefore $e_y = e_2 + D_2f_s$. It follows that

$$\dot{e}_1 = \tilde{A}_1e_1 + He_y - HD_2f_s - K_1v \tag{23}$$

$$\dot{e}_y = A_3e_1 - K_2e_y + K_2D_2f_s - K_3v + D_2\dot{f}_s \tag{24}$$

Then, introduce a new coordinate transformation $\text{col}(e_1e_y) \rightarrow (e_se_y)$ with $e_s = e_1 + \Gamma e_y$, where Γ will be defined later. The error systems in (23)–(24) become

$$\dot{e}_s = (\tilde{A}_1 + \Gamma A_3)e_s + [H - \Gamma K_2 - (\tilde{A}_1 + \Gamma A_3)\Gamma]e_y - (K_1 + \Gamma K_3)v - (H - \Gamma K_2)D_2f_s + \Gamma D_2\dot{f}_s \tag{25}$$

$$\dot{e}_y = A_3e_s - (K_2 - A_3\Gamma)e_y - K_3v + K_2D_2f_s + D_2\dot{f}_s \tag{26}$$

For the system (25), and as a direct result of Lemma 1 under Assumption 2, there exists a matrix Γ such that $(\tilde{A}_1 + \Gamma A_3)$ with $\tilde{A}_1 = (A_1 + LA_3)$ is the Hurwitz matrix, where L is defined in Lemma 1. Thus, for any $\tilde{Q} \succ 0$ the Lyapunov equation

$$(\tilde{A}_1 + \Gamma A_3)^T \tilde{P}_1 + \tilde{P}_1(\tilde{A}_1 + \Gamma A_3) = -\tilde{Q}_1 \tag{27}$$

has an unique solution $\tilde{P} \succ 0$.

With the selection of $H = [\Gamma K_2 + (\tilde{A}_1 - \Gamma A_3)\Gamma]$ and $K_1 = -\Gamma K_3$, the system (25) becomes

$$\dot{e}_s = (\tilde{A}_1 - \Gamma A_3)e_s - (H - \Gamma K_2)D_2 f_s + \Gamma D_2 \dot{f}_s \tag{28}$$

Considering the Lyapunov candidate function $V = e_s^T \tilde{P}_1 e_s$, and from (27)

$$\dot{V} = -e_s^T \tilde{Q}_1 e_s - 2\tilde{P}_1 e_s^T [(H + \Gamma K_2)D_2 f_s - \Gamma D_2 \dot{f}_s] \tag{29}$$

From Assumption 1

$$\begin{aligned} \dot{V} &\leq -\underset{\min}{\lambda}(\tilde{Q}_1)\|e_s\|^2 - 2\left\|\tilde{P}_1\right\|\|e_s\|\,\|[(H + \Gamma K_2)D_2\beta_1 - \Gamma D_2\beta_2]\| \\ &\leq -(\frac{1}{2}\underset{\min}{\lambda}(W^T + W)\|\mathrm{X}\| + \gamma)\|\mathrm{X}\| \end{aligned} \tag{30}$$

where $W = \tilde{Q}_1$, $X = e_s$ and $\gamma = 2\left\|\tilde{P}_1\right\|\|[(H + \Gamma K_2)D_2\beta_1 - \Gamma D_2\beta_2]\|$. From the definition of Lyapunov function in (27), it is straightforward to see that

$$\underset{min}{\lambda}(\tilde{P}_1)\|X\|^2 \leq V \leq \underset{max}{\lambda}(\tilde{P}_1)\|X\|^2 \tag{31}$$

Therefore, system (25) is globally uniformly ultimately bounded. Hence the result follows.

Remark 1. From the above result, it follows that e_s is bounded and thus there exist constant $\alpha \succ 0$ such that

$$\|e_s\| \leq \alpha \tag{32}$$

where α can be estimated using the approach given in [20].

For the system (25)–(26), consider the sliding surface

$$S = \{\mathrm{col}(e_s, e_2)|e_2 = 0\} \tag{33}$$

Then the following conclusion is ready to be presented.

Theorem 1. *Under Assumptions 1–2, system (25)–(26) is driven to the sliding surface (33) in finite time and remains on it if*

$$K_3 \geq \|A_3\|\alpha + \|K_2D_2\|\beta_1 + \|D_2\|\beta_2 + \eta \tag{34}$$

Proof. From (26) with selection of $K_2 = A_3\Gamma$, and from Assumption 1, it follows that

$$\begin{aligned} e_y^T\dot{e}_y &= e_y^T[A_3e_s - K_3v + K_2D_2f_s + D_2\dot{f}_s] \\ &\leq e_y^T[A_3e_s + K_2D_2\beta_1 + D_2\beta_2 - K_3v] \end{aligned} \tag{35}$$

From Remark 1, and from the inequality $\|X\| \leq X^T sgn(X)$

$$\begin{aligned} e_y^T\dot{e}_y &\leq [\|A_3\|\alpha\left\|e_y\right\| + \|K_2D_2\|\beta_1\left\|e_y\right\| + \|D_2\|\beta_2\left\|e_y\right\| - \|K_3\|\left\|e_y\right\|] \\ &\leq [\|A_3\|\alpha + \|K_2D_2\|\beta_1 + \|D_2\|\beta_2 - \|K_3\|]\left\|e_y\right\| \end{aligned} \tag{36}$$

Applying (34) into (36)

$$e_y^T\dot{e}_y \leq -\eta\left\|e_y\right\| \tag{37}$$

This shows that the reachability condition is satisfied. Hence the conclusion follows.

After sliding motion occurs $e_2 = \dot{e}_2 = 0 \Rightarrow e_s = e_1$. Thus

$$\underset{t\to\infty}{lim}\, e_s = 0, \underset{t\to\infty}{lim}\, e_1 = 0 \tag{38}$$

Thus, From (38), and for slowly varying faults if the dynamics of the sliding motion are sufficiently fast

$$0 = A_3 e_s - K_3 v + K_2 D_2 f_s + D_2 \dot{f}_s$$
$$v_{eq} \to K_3^{-1} \| K_2 D_2 \| f_s(t) \tag{39}$$

In order to reconstruct/estimate the fault signal $f_s(t)$, it is necessary to recover the equivalent output error injection signal v_{eq}. Here the approach given in [21] and later in [22] will be employed to produce the v_{eq}. From (18), the equivalent output error injection signal v_{eq} can be approximated by

$$v_{eq} \simeq \frac{e_y}{\|e_y\| + \sigma} \tag{40}$$

where σ is a small positive scalar. It can be shown that the equivalent output injection can be approximated to any degree of accuracy by (40) for a small enough choice of σ. Since rank D_2, it follows from (39) that

$$f_s(t) \simeq (K_3^{-1} \| K_2 D_2 \|)^{-1} \frac{e_y}{\|e_y\| + \sigma} \tag{41}$$

Remark 2. In the following simulation studies $q = 1 (D_2 = 1)$ (one output voltage sensor for voltage model, and one output temperature sensor for thermal model). From (41), it is clear that the estimation of fault signal is only dependent on y and $\widehat{y}$ which can be obtained online. Therefore, the fault estimation scheme is convenient for real implementation.

4. Simulation studies

The observer developed in this paper is applied to validated voltage model that represents a real cell of a Nissan Leaf Gen4 Li-ion battery, and it is used alongside with a thermal battery cell model. Both models are developed at The University of Warwick-WMG.

4.1. Simulation using voltage model

The matrices (A, B, C) in (4)–(5) of voltage model that described in [19] are used in this paper to implement the observer in (15)–(17) for voltage cell.

All parameters and states definitions are explained in [19]. Different well known drive cycle profiles; New European Driving Cycle (NEDC), and more recently the Worldwide Harmonised Light Vehicle Test Procedure (WLTP) are used in the simulation. Nissan Leaf Gen4 2018 Lithium-ion cell model has been characterised in the lab, and the data obtained is used to develop Lithium-ion cell model. The observer developed in this paper is used to estimate the unmeasurable states of the voltage model (OCV, V_{pe}, V_{pc}) (see Fig. 2) and the fault signal.

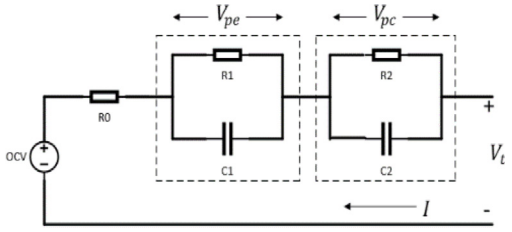

Fig. 2. A second-order equivalent circuit model for battery cell represents the system states.

Figs. 3-a and 4-a show the simulation results of the full system states (V_t, OCV, V_{pe}, V_{pc}) (see Fig. 2) under NEDC and WLTP current profiles respectively. It can be seen that although the high frequency of the current profiles, the estimation signals still follow the systems states in good manner.

Figs. 3-b and 4-b show fault signals estimation at different formats; First, when the simulated fault signal is dropped suddenly to -1 (e.g., sensor broken); Second, when the simulated fault signal is considered as a pulse signal with -1 amplitude (e.g., sensor with bad contact).

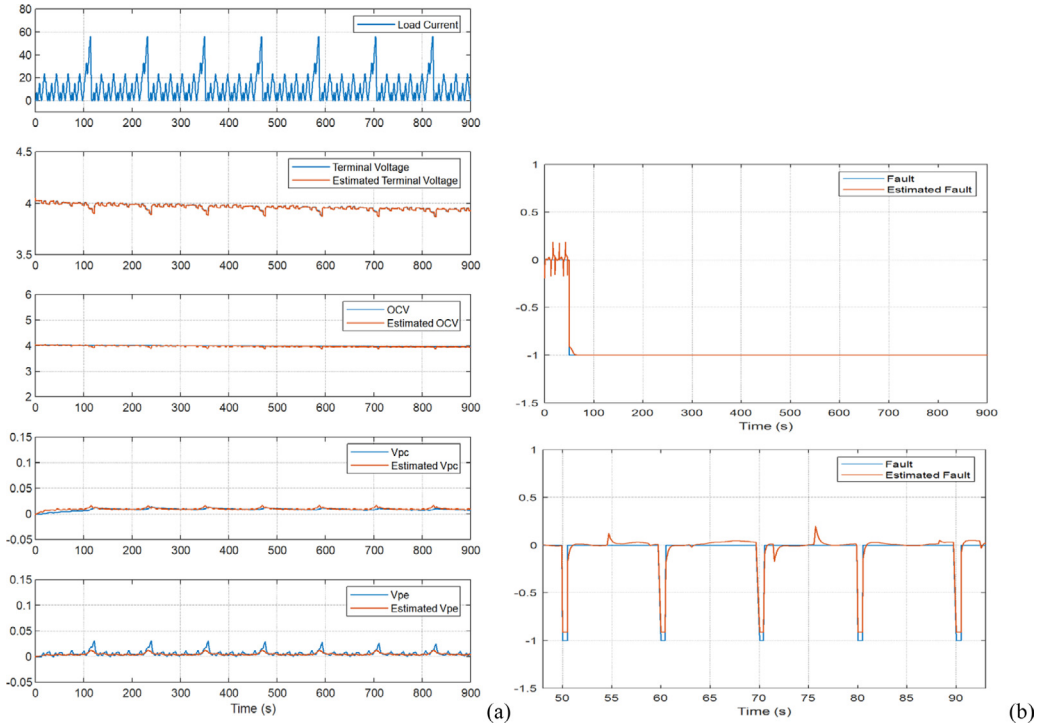

Fig. 3. (a) System states estimation-NEDC; (b) Different formats of fault signals: Top; fault signal simulation drops to −1. Bottom; Pulse with −1 amplitude fault signal.

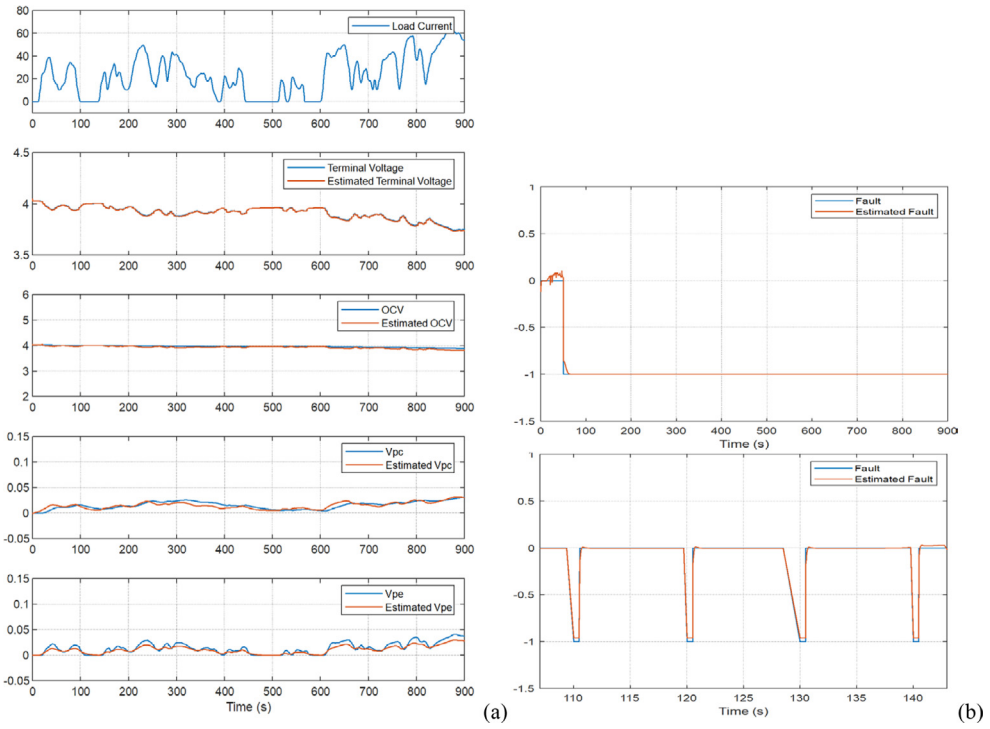

Fig. 4. (a) System states estimation-WLTP; (b) Different formats of fault signals: Top; fault signal simulation drops to −1. Bottom; Pulse with −1 amplitude fault signal.

4.2. Simulation using thermal model

The matrices (A, B, C) in (4)–(5) of thermal model that described in [18] is used in this paper to implement the observer in (15)–(17) for battery cell thermal model. The matrices (A, B, C) of the thermal model are in the form:

$$A = \begin{bmatrix} \frac{-1}{R_c C_c} & \frac{1}{R_c C_c} \\ \frac{1}{R_c C_s} & \frac{-1}{C_s}\left(\frac{1}{R_c} + \frac{1}{R_u}\right) \end{bmatrix}, \quad B = \begin{bmatrix} \frac{R_e R_c}{C_c} & 0 \\ 0 & \frac{1}{R_u C_s} \end{bmatrix}, \quad C = [0 \quad 1] \tag{42}$$

where $x = [T_c T_s]^T$ and $u = [I^2 T_f]$, T_c is a core temperature, T_s is a surface temperature, I is a current, and T_f is an ambient temperature. The parameters of the thermal model can be found in [18]. The same procedures done for voltage model that mentioned above, they were done for the thermal model in terms of different drive cycles and different fault formats.

Figs. 5-a and 6-a show the simulation results of the full system states $x = [T_c \quad T_s]^T$ under NEDC and WLTP current profiles respectively. Figs. 5-b and 6-b show fault signals estimation at different formats; First, when the simulated fault signal is dropped suddenly to -1 (e.g., sensor broken); Second, when the simulated fault signal is considered as a pulse signal with -1 amplitude (e.g., sensor with bad contact).

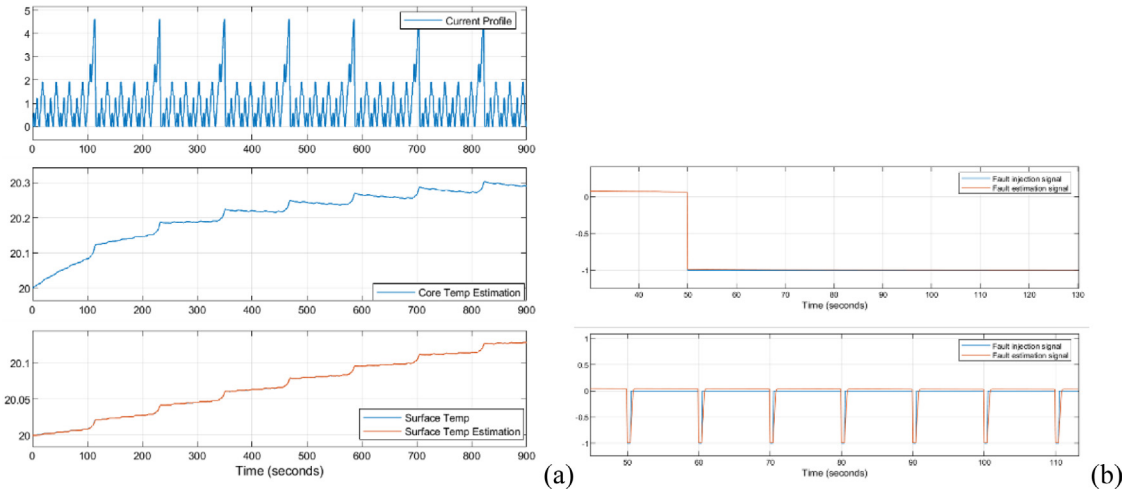

Fig. 5. (a) System states estimation-NEDC. (b) Different forms of fault signals; Top: fault signal simulation drops to -1. Bottom: pulse signal with -1 amplitude.

Remark 3. It can be seen that in all the scenarios mentioned above for both models (voltage and thermal models of the battery cell), the system states and fault signals have been effectively estimated. In addition, the well-known issue which is the internal short circuit that might causes very serious problems can be indicated by the estimation of the core temperature, as it is very difficult to be measured, and the terminal voltage drop at the same time.

5. Conclusion

In this paper, a sliding mode observer has been considered to estimate the Li-Ion battery voltage and thermal cell system states as well as sensor fault estimation. The developed virtual voltage model that represents Nissan Leaf Gen4 Li-ion battery cell and virtual thermal model are used as applications to perform the estimation process. Different current profiles and different fault signals format are used to show the reliability of the proposed technique. The internal short circuit could be indicated if the monitoring shows a terminal voltage drop and a rapid increase of the core temperature estimation simultaneously.

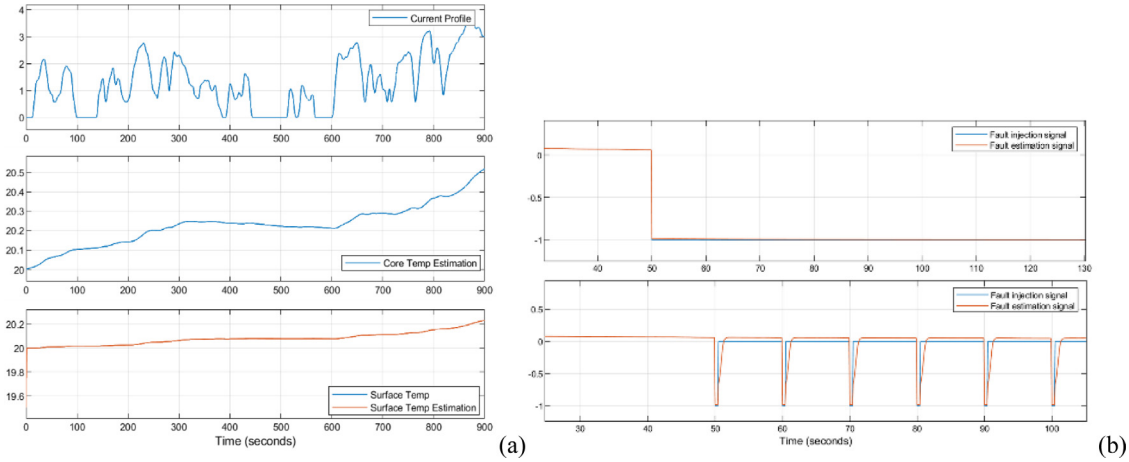

Fig. 6. (a) System states estimation-WLTP. (b) Different forms of fault signals; Top: fault signal simulation drops to -1. Bottom: pulse signal with -1 amplitude.

Declaration of competing interest

The authors declare that they have no known competing financial interests or personal relationships that could have appeared to influence the work reported in this paper.

Data availability

No data was used for the research described in the article.

Acknowledgements

This work was supported by Smart Efficient Energy Centre (SEEC) at Bangor University, UK, part-funded by the European Regional Development Fund (ERDF), administered by the Welsh Government.

References

[1] J. Jiang, C. Zhang, Fundamentals and applications of lithium-ion batteries in electric drive vehicles, John Wiley & Sons, 2015.
[2] C. Mikolajczak, M. Kahn, K. White, R.T. Long, Lithium-ion batteries hazard and use assessment, Springer Science & Business Media, 2012.
[3] X. Zhang, C. Mi, Vehicle power management: Modeling, control and optimization, Springer Science & Business Media, 2011.
[4] A.P. Fire, Boston, massachusetts: JA829j, Jpn Airl Boeing (2014) 787–788.
[5] S. Saxena, L. Kong, M.G. Pecht, Exploding e-cigarettes: A battery safety issue, IEEE Access 6 (2018) 21442–21466.
[6] M. Lelie, T. Braun, M. Knips, H. Nordmann, F. Ringbeck, H. Zappen, D.U. Sauer, Battery management system hardware concepts: An overview, Appl Sci 8 (4) (2018) 534.
[7] X. Feng, M. Ouyang, X. Liu, L. Lu, Y. Xia, X. He, Thermal runaway mechanism of lithium ion battery for electric vehicles: A review, Energy Storage Mater 10 (2018) 246–267.
[8] G.H. Kim, K. Smith, J. Ireland, A. Pesaran, Fail-safe design for large capacity lithium-ion battery systems, J Power Sources 210 (2012) 243–253.
[9] J. Zhang, A.K. Swain, S.K. Nguang, Robust observer-based fault diagnosis for nonlinear systems using MATLAB®, Springer, Berlin, 2016, p. 224.
[10] H. Alwi, C. Edwards, C.P. Tan, Fault detection and fault-tolerant control using sliding modes, Springer, London, 2011, pp. 7–28.
[11] X.G. Yan, S.K. Spurgeon, C. Edwards, Variable structure control of complex systems, Commun Control Eng (2017).
[12] C. Edwards, S. Spurgeon, Sliding mode control: Theory and applications, Crc Press, 1998.
[13] V.I. Utkin, Sliding modes in control and optimization, Springer Science & Business Media, 2013.
[14] S. Dey, S. Mohon, P. Pisu, B. Ayalew, Sensor fault detection, isolation, and estimation in lithium-ion batteries, IEEE Trans Control Syst Technol 24 (6) (2016) 2141–2149.
[15] Z. Liu, H. He, Sensor fault detection and isolation for a lithium-ion battery pack in electric vehicles using adaptive extended Kalman filter, Appl Energy 185 (2017) 2033–2044.
[16] M.K. Tran, M. Fowler, Sensor fault detection and isolation for degrading lithium-ion batteries in electric vehicles using parameter estimation with recursive least squares, Batteries 6 (1) (2019) 1.

[17] R. Xiong, Q. Yu, W. Shen, C. Lin, F. Sun, A sensor fault diagnosis method for a lithium-ion battery pack in electric vehicles, IEEE Trans Power Electron 34 (10) (2019) 9709–9718.
[18] X. Lin, H.E. Perez, J.B. Siegel, A.G. Stefanopoulou, Y. Li, R.D. Anderson, M.P. …Castanier, Online parameterization of lumped thermal dynamics in cylindrical lithium ion batteries for core temperature estimation and health monitoring, IEEE Trans Control Syst Technol 21 (5) (2012) 1745–1755.
[19] X. Chen, W. Shen, Z. Cao, A. Kapoor, A novel approach for state of charge estimation based on adaptive switching gain sliding mode observer in electric vehicles, J Power Sources 246 (2014) 667–678.
[20] X.G. Yan, C. Edwards, Robust sliding mode observer-based actuator fault detection and isolation for a class of nonlinear systems, Internat J Systems Sci 39 (4) (2008) 349–359.
[21] C. Edwards, S.K. Spurgeon, R.J. Patton, Sliding mode observers for fault detection and isolation, Automatica 36 (4) (2000) 541–553.
[22] X.G. Yan, C. Edwards, Nonlinear robust fault reconstruction and estimation using a sliding mode observer, Automatica 43 (9) (2007) 1605–1614.